The Eurasia Proceedings of Science, Technology, Engineering & Mathematics (EPSTEM)
ISSN: 2602-3199

The Eurasia Proceedings of Science, Technology, Engineering & Mathematics (EPSTEM), 2022

Volume 21, Pages 484-499

IConTES 2022: International Conference on Technology, Engineering and Science

An Analysis of Flexural Bond Length and Anchorage Length of Prestressed Fiber Reinforced Polymer Reinforcement

Aidas JOKŪBAITIS
Vilnius Gediminas Technical University

Juozas VALIVONIS
Vilnius Gediminas Technical University

Abstract: The main aim of this paper is to provide a broader analysis of the flexural bond length and anchorage length of different types of prestressed Fiber Reinforced Polymer (FRP) reinforcement and to provide corrections to the existing theoretical models. Therefore, this paper presents a description of the main parameters that influence the flexural bond length and anchorage length of different types of FRP reinforcement based on experimental results found in the literature. The database of more than 70 specimens was compiled with the results of the transfer length, flexural bond length, and anchorage length of FRP reinforcement and the main influencing parameters. The analysis of a larger database of flexural bond length revealed that propositions of coefficients α_{fb} = 2.8 and α_{fb} = 1.0 found in the literature for Carbon Fiber Composite Cable (CFCC) strands and Carbon Fiber Reinforced Polymer (CFRP) bars, respectively, should be corrected. Therefore, corrected values of coefficient α_{fb} are proposed in this article for CFCC strands (α_{fb} = 3.0) and CFRP bars (α_{fb} = 0.9). Additionally, the new value of α_{fb} = 1.4 is proposed for flexural bond length of Aramid Fiber Reinforced Polymer (AFRP) bars. Moreover, the main existing theoretical models are presented, and the comparison of theoretical and experimental flexural bond length and anchorage length results is discussed. Additionally, the analysis of the flexural bond length and anchorage length and the proposed new values of the coefficient α_{fb} provides possibilities for adapting it to design codes for engineering applications and performing additional research that fills the missing gaps in the field.

Keywords: Prestress, Fiber reinforced polymer, Flexural bond length, Anchorage length, Bond

Introduction

The corrosive environment of such structures as marine structures, bridges, parking garages, and railway sleepers (Jokūbaitis et al., 2020b; Jokūbaitis, Marčiukaitis, et al., 2016; Jokūbaitis, Valivonis, et al., 2016) is the main concern with regard to steel corrosion (deicing salts, etc.). Therefore, there is increasing interest in the use of FRP materials, namely, CFRP, AFRP, GFRP, and relatively new BFRP (E. Atutis et al., 2018; M. Atutis et al., 2018) as replacements for steel reinforcement.

FRPs have important properties that make them particularly attractive for prestressed concrete applications: high strength, which is similar to or greater than that of steel, and low modulus of elasticity, which results in lower concrete prestress losses due to concrete creep and shrinkage as well as the relaxation of the prestressing element. The major difficulty in using FRP reinforcement for prestressing is that anchorage systems require greater attention than those for steel strands. Therefore, three types of anchorage systems are developed for FRP reinforcement: mechanical, bonded, and composite (Wang et al., 2018).

The use of FRP reinforcement in prestressed concrete structures is highly dependent on the reliability of the reinforcement anchorage zone. That is, the behavior of concrete members is mainly dependent on the bond between reinforcement and concrete (Jokūbaitis et al., 2017, 2018, 2020a). Combinations of several factors have been shown to contribute to the bond of pretensioned reinforcement to concrete. Depending on the circumstances, adhesion, Hoyer effect, and mechanical interlocking can act alone or in combination to resist slip of reinforcement in concrete. While adhesion is weak, mechanical interlock and friction create higher bond strength and are quite dependent on the surface characteristics of the reinforcement.

The pretension technique relies on the bond between the prestressing reinforcement and the surrounding concrete to transfer the stresses from the prestressing reinforcement to the concrete. Figure 1 provides a curve illustrating the variation in reinforcement stresses along the length of the flexural member starting from the free end of the strand. Transfer length (L_t) is defined as the length from the free end of the member to the point along the length of the beam where the effective prestress in the strand is fully transferred to the concrete during reinforcement release. The stress in the strand along the length of the transfer length is assumed to vary linearly from zero at the free end to an effective prestress after losses (f_{pe}) at the end of the transfer length. The flexural bond length (L_{fb}) is defined as the length of a fully bonded reinforcement beyond the transfer length required to fully develop the stress in the reinforcement to the maximum stress (f_{pu}) at the flexural bearing capacity, when load is applied to the member. Anchorage length (L_a) is the sum of the transfer length (L_t) and the flexural bond length (L_{fb}). Transfer length, flexural bond length, and development length are illustrated in Figure 1.

The transfer and development length of an FRP reinforcement is a function of the perimeter and surface condition of the FRP, the stress in the FRP, the method used to transfer the force of the FRP to the concrete and the strength and cover of the concrete. The mechanism of the bond differs between FRP and steel strands due to differences in shape, surface treatment, and modulus of elasticity. FRP reinforcement may be produced using unique manufacturing processes, which result in different properties and configurations of the reinforcement surface. The stronger the bond strength, the shorter the length required to transfer a certain amount of stress between the reinforcement and the concrete. Therefore, the strand length required to transfer the effective prestress and develop its ultimate strength should be predicted with careful consideration. At any point along the section, the loss of the bond between the reinforcement and concrete can lead to sudden failure: due to splitting failure or pull-out failure.

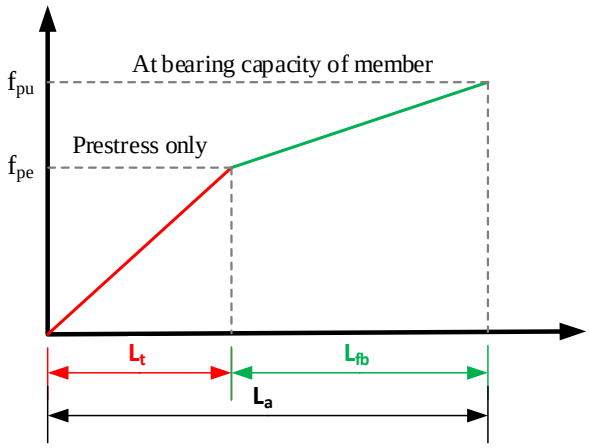

Figure 1. Anchorage zone of pretensioned reinforcement

In the last 30 years, numerous experimental researchers have investigated the transfer, flexural bond, and anchorage lengths of different prestressed FRP reinforcements. The large variation of different FRP types leads to the need for experimental research. Therefore, some studies were performed to investigate the transfer, flexural bond, and anchorage length of CFCC strands (Domenico, 1995; Domenico et al., 1998; Ehsani et al., 1997; Mahmoud, 1997; Mahmoud et al., 1999), CFRP bars (Dolan et al., 2001; Ehsani et al., 1997; Krem, 2013; Krem et al., 2018; Lu et al., 2000; Mahmoud, 1997; Mahmoud et al., 1999) and AFRP bars (Dolan et al., 2001; Ehsani et al., 1997; Lu et al., 2000; Nanni et al., 1992; Nanni & Tanigaki, 1992). However, the large variation in FRP bars in terms of shape, surface conditions, strength, and modulus of elasticity indicates that a deeper understanding of the transfer and flexural bond length of FRPs with different properties remains necessary. Therefore, this article presents a database of transfer, flexural bond, and anchorage length results for pretensioned FRP reinforcement and provides a comparative analysis of the anchorage zones of different types of FRP.

Theoretical Models

Table 1 presents a summary of the recommended expressions for the transfer and flexural bond lengths of the FRP reinforcement (Equations (1), (2), (6), (7), and (8)) and the steel strands (Equations (3), (4), (5), (9) and (10)). The nomenclature is presented in this table. The transfer length equations (Table 1) are discussed in detail in (Jokūbaitis et al., 2022).

Equations (4) and (9) provided in (ACI 318-11, 2011) evaluate the fewest different parameters (f_{pi}, f_{pe}, f_{pu}, and Ø) that influence the transfer length and flexural bond length. Additionally, with an empirical coefficient of 20.7 and 0.145, which are based on the large database of transfer and flexural bond length results, respectively, Equations (3), (4) and (9) were developed for steel strands. Lu et al. (Lu et al., 2000) modified Equation (8) provided in (ACI 318-11, 2011) for the flexural bond length of FRP reinforcement. However, the modified Equation 8 gives a conservative prediction of the experimental results. In addition, Mitchell et al. (Mitchell et al., 1993) suggested supplementing the ACI-318-11 (ACI 318-11, 2011) Equations (4) and (9) with the concrete compressive strength at the transfer and in service stages. As concrete strength enhances the bond of reinforcement, it becomes a good additional parameter to increase the accuracy of the transfer length and the prediction of the flexural bond length. However, Equations (4) and (9) are proposed for the steel strands. Compared with Equations (1) and (6), Equations (2) and (7) proposed by Domenico (Domenico, 1995) replace the reinforcement diameter (Ø) with a cross-sectional area (A_p) of the reinforcement and propose empirical coefficients $C_t = 80$ and $C_{fb} = 40$ for the transfer and flexural bond lengths of the CFCC strand, respectively. Additionally, it evaluates $f_{ci}^{1/2}$ and $f_c^{1/2}$ as also in Equations (5) and (10), respestively.

Table 1. Theoretical models of transfer and flexural bond length

References	Transfer length	Equation No	Flexural bond length	Equation No	Notes
(Mahmoud, 1997)	$L_t = \frac{f_{pi} \cdot \varnothing}{\alpha_t \cdot f_{ci}^{\frac{2}{3}}}$	(1)	$L_{fb} = \frac{\left(f_{pu} - f_{pe}\right) \cdot \varnothing}{\alpha_{fb} \cdot f_c^{\frac{2}{3}}}$	(6)	f_{pi} - is the initial prestress level, f_{pe} – effective prestressing stress in the CFCC strand, f_{pu} stress at first slip or at rupture of reinforcement, f_{ci} - is the concrete compressive strength at the time of transfer, f_c concrete compressive strength at the time of testing, Ø - is the reinforcement diameter, A_p – cross-sectional area of prestressed reinforcement, α_t and α_{fb} - is a material dependent coefficient, C_T – constant is equal to 80 for CFCC strands, C_{fb} constant is equal to 40 for CFCC strands.
(Domenico, 1995)	$L_t = \frac{f_{pe} \cdot A_p}{C_T \cdot \sqrt{f_{ci}}}$	(2)	$L_{fb} = \frac{\left(f_{pu} - f_{pe}\right) \cdot A_p}{C_{fb} \cdot \sqrt{f_c}}$	(7)	
(Lu et al., 2000)	$L_t = \frac{f_{pi} \cdot \varnothing}{20.7}$	(3)	$L_{fb} = 0.10875 \cdot \left(f_{pu} - f_{pe}\right) \cdot \varnothing$	(8)	
(ACI 318-11, 2011)	$L_t = \frac{f_{pi} \cdot \varnothing}{20.7}$	(4)	$L_{fb} = 0.145 \cdot \left(f_{pu} - f_{pe}\right) \cdot \varnothing$	(9)	
(Mitchell et al., 1993)	$L_t = \frac{f_{pi} \cdot \varnothing}{20.7} \cdot \sqrt{\frac{20.7}{f_{ci}}}$	(5)	$L_{fb} = 0.145 \cdot \left(f_{pu} - f_{pe}\right) \cdot \varnothing \cdot \sqrt{\frac{30}{f_c}}$	(10)	

Equations (1) and (6) were proposed by (Mahmoud, 1997; Mahmoud et al., 1999) for CFRP Leadline bars and CFCC strands and were adopted in several design codes (ACI 404.4R-04, 2004; CAN-CSA S806-12, 2012). It takes into account reinforcement diameter (Ø), stresses in reinforcement (f_{pi}, f_{pe}, f_{pu}), and concrete compressive strength (f_{ci}, f_c). The main difference from other theoretical models is that Equations (1) and (6) propose empirical coefficients α_t and α_{fb}, respectively, depending on the type of FRP reinforcement. Therefore, these coefficients can be calibrated for different types of FRP reinforcement (GFRP, CFCC, CFRP, AFRP, BFRP) with different surface conditions. Additionally, it presents the concrete strength as $f_c^{2/3}$ instead of $f_c^{1/2}$ (Equations (2), (5), (7), and (10)). The presentation of concrete strength as $f_c^{2/3}$ can be explained by the correlation of concrete compressive strength with concrete tensile strength $f_{ctm} = 0.3 \cdot f_c^{2/3}$ provided in (EN 1992-1-1, 2004; MC 1990, 1991; MC 2010, 2012).

Table 2 presents the values of coefficients α_t, α_{fb}, C_t, and C_{fb} provided in Equations (1), (6), (2), and (7), respectively, for different types of FRP reinforcement found in the literature. Domenico (Domenico, 1995) proposed empirical coefficients $C_t = 80$ and $C_{fb} = 40$ for the transfer and flexural bond lengths of the CFCC strand, respectively. The values proposed by (Mahmoud, 1997; Mahmoud et al., 1999) and adopted in (ACI 404.4R-04, 2004; CAN-CSA S806-12, 2012) are $\alpha_t = 1.9$, $\alpha_{fb} = 1.0$ and $\alpha_t = 4.8$, $\alpha_{fb} = 2.8$ for CFRP Leadline bars and CFCC strands, respectively. Additionally, (Krem, 2013; Krem et al., 2018) investigated specimens made of self-compacting concrete (SCC) and prestressed with CFRP bars and proposed $\alpha_t = 2.84f_{pi}/800$, $\alpha_{fb} = 0.37+(f_{pu}-f_{pe})/2500$.

Table 2. Theoretical models of transfer and flexural bond length

References	Reinforcement Type	Transfer length	Flexural bond length
(Mahmoud, 1997; Mahmoud et al., 1999)	CFRP Leadline bars	$\alpha_t = 1.9$	$\alpha_{fb} = 1.0$
	CFCC strands	$\alpha_t = 4.8$	$\alpha_{fb} = 2.8$
(Domenico, 1995; Domenico et al., 1998)	CFCC strands	$C_t = 80$	$C_t = 40$
(Krem, 2013; Krem et al., 2018)	CFRP bars (SCC concrete)	$\alpha_t = 2.84\text{-}f_{pi}/800$	$\alpha_{fb} = 0.37+(f_{pu}\text{-}f_{pi})/2500$
(Jokūbaitis & Valivonis, 2022)	AFRP smooth braided bars	$\alpha_t = 1.5$	–
	AFRP rough and sanded bars	$\alpha_t = 4.0$	–

Results

The Database of the Results

A literature review of the transfer length, flexural bond length, and anchorage length of concrete specimens pretensioned with different FRP reinforcement was performed. The results of 106 beams were collected (Annex A). The ranges of the initial parameters of the database are provided in Table 3. A literature review revealed that prestressed concrete flexural members tested for flexural bond and anchorage lengths showed flexural failure or reinforcement anchorage failure (Mahmoud, 1997; Mahmoud et al., 1999; Nanni & Tanigaki, 1992). The flexural member can be designed to fail either in the concrete compressive zone (Nanni & Tanigaki, 1992) or by reinforcement rupture (Mahmoud, 1997; Mahmoud et al., 1999). The flexural bond and anchorage lengths can be determined when the beam failure is between the flexural failure and the reinforcement anchorage failure. Therefore, for the analysis of the flexural bond and anchorage lengths, only the results of beams that failed between flexural failure and reinforcement anchorage failure were taken into account. Specifically, 16 of 36, 16 of 36, and 21 of 34 specimens prestressed with CFCC (Table A1), CFRP (Table A2), and AFRP (Table A3) reinforcement were used for the analysis, respectively. Tables A1-A3 (Annex A) provide original markings of specimens from the experimental research, type and surface conditions of FRP reinforcement, specimen type, concrete protective cover (c), reinforcement diameter (Ø), cross-sectional area of the bar (A_p), modulus of elasticity of reinforcement (E_p), concrete compressive strength at the time of testing (f_c), effective stresses in reinforcement taking into account losses of prestress (f_{pe}), stress at first slip or at rupture of reinforcement (f_{pu}), transfer length (L_t), flexural bond length (L_{fb}), anchorage length (L_a) and mode of failure of beam.

Table 3. Summary of initial parameters of the database

FRP Type	c, mm	Ø, mm	A_p, mm^2	E_p, GPa	f_{pu}, MPa	f_{pe}, MPa	f_c, MPa
CFCC	45–75	10.5–15.2	55.7–113.6	137–141	1734–2305	735–1306	31–64
CFRP	35–40.6	7.9–12.7	46.1–126.7	144–171	1360–3000	535–1400	37–70.9
AFRP	40.6–66	7.4–16	38.1–1802	45–127	1021–2448	258–1061	31–47.1

Derivation of Coefficient α_{fb}

The most widely used equation (Equation (6)) for the flexural bond length of the pretensioned FRP reinforcement is proposed by (Mahmoud, 1997; Mahmoud et al., 1999) and is adopted in design codes (ACI 404.4R-04, 2004; CAN-CSA S806-12, 2012). Additionally, it takes into account the reinforcement diameter (Ø), concrete compressive strength (f_c), stresses in reinforcement (f_{pe}, f_{pu}) and material dependent coefficient (α_{fb}), which are one of the main parameters that influence the flexural bond length of pretensioned FRP reinforcement. Therefore, for a better analysis of the results based on Equation (6), a graphical comparison of

the flexural bond length of different FRP reinforcements (CFCC, CFRP, and AFRP) and $\left(f_{pu}-f_{pe}\right)\cdot\varnothing/f_c^{2/3}$ is presented in Figure 2. Additionally, these graphs (Figure 2) represent a distribution of the results with the proposed mean values of the coefficient α_{fb}. For the CFCC strand database, the average value of the coefficient α_{fb} is 3.0 with a standard deviation (STD) of 0.62 and a coefficient of variation (COV) of 20.5% (Table 4) (for concrete strength 31–64 MPa, effective prestress 735–1306 MPa, stresses at failure 1734–2305 MPa and reinforcement diameter 10.5–15.2 mm).

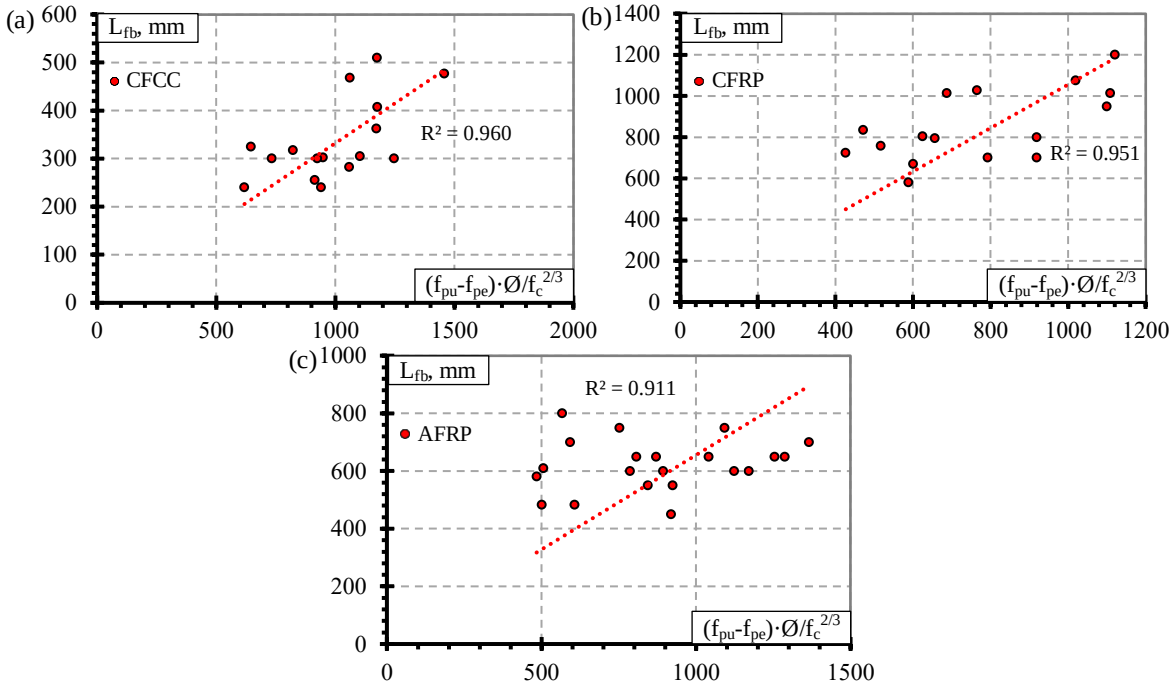

Figure 2. Relationship between flexural bond length and $\left(f_{pu}-f_{pe}\right)\cdot\varnothing/f_c^{2/3}$ of (a) CFCC strands, (b) CFRP bars, and (c) AFRP bars

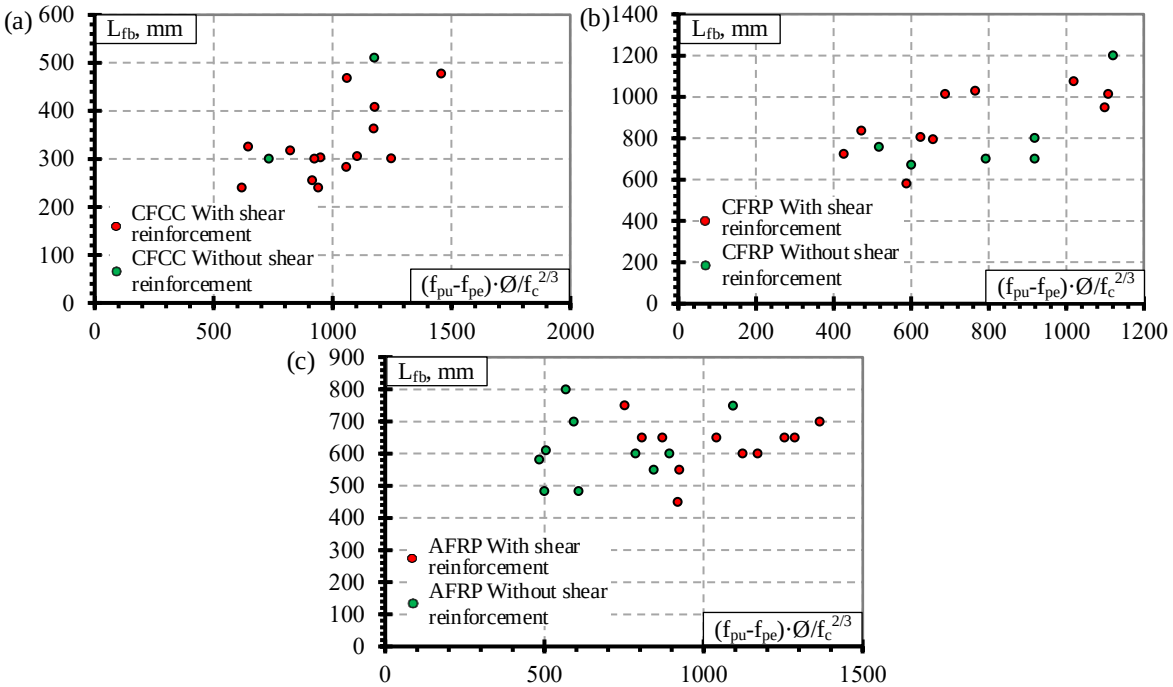

Figure 3. Relationship between flexural bond length and $\left(f_{pu}-f_{pe}\right)\cdot\varnothing/f_c^{2/3}$ of (a) CFCC strands, (b) CFRP bars, and (c) AFRP bars

The graphical representation is presented in Figure 2a with a very strong correlation coefficient $R^2 = 0.96$. Figure 2b presents the relationship between flexural bond length and $\left(f_{pu} - f_{pe}\right) \cdot \varnothing / f_c^{2/3}$ with an average $\alpha_{fb} = 0.9$ with STD = 0.22, COV = 24.0%, and $R^2 = 0.95$ (Table 4) (for concrete strength 37–71 MPa, effective prestress 535–1400 MPa, stress at failure 1360–3000 MPa, and reinforcement diameter 7.9–12.7 mm). Figure 2c presents the transfer length distribution of the AFRP bars with respect to $\left(f_{pu} - f_{pe}\right) \cdot \varnothing / f_c^{2/3}$ with an average $\alpha_{fb} = 1.4$ with STD = 0.42, COV = 29.8%, and $R^2 = 0.91$ (Table 4) (for concrete strength 31–47 MPa, effective prestress 258–1061 MPa, stress at failure 1021–2448 MPa, and reinforcement diameter 7.4–16 mm).

Table 4. Results of coefficient α_{fb}

α_{fb}	CFCC (Mahmoud, 1997)	Proposed	CFRP (Mahmoud, 1997)	Proposed	AFRP Proposed
Mean	2.8	3.0	1.0	0.9	1.4
Standard deviation	-	0.62	-	0.22	0.42
Coefficient of variation, %	-	20.5	-	24.0	29.8

In the database (Annex A) all CFCC strands had a helical plain surface, CFRP bars had a spirally indented (Leadline) or sanded surface, and AFRP bars had a smooth braided or rough surface. However, there were no clear influence of different reinforcement surface conditions on the flexural bond length of prestressed FRP reinforcement. Additionally, Figure 3 shows the influence of shear reinforcement on the relationship between flexural bond length and $\left(f_{pu} - f_{pe}\right) \cdot \varnothing / f_c^{2/3}$. It is clear that there is no clear influence of shear reinforcement on the flexural bond length of CFCC strands (Figure 3a), CFRP bars (Figure 3b), and AFRP bars (Figure 3c). However, Mahmoud (Mahmoud, 1997) determined that the absence of shear reinforcement resulted in an increase of the flexural bond length by 25% compared with specimens with shear reinforcement. This was explained by the helical shape of CFCC seven-wire strand which activates the confining of shear reinforcement due to higher radial stresses than that in the case of CFRP Leadline bar. Furthermore, concrete protective cover also plays an important role, in that the deeper the cover around the tendon, the less likely is the propagation of split (Nanni & Tanigaki, 1992).

Comparison of Experimental and Theoretical Results

In this section, the theoretical models for the calculation of transfer length, flexural bond length, and anchorage length (Table 1) are compared with experimental results from the literature (Tables A1–A3). The results presented in Figures 4 and 5 show the relationships between the experimental and theoretical results of the transfer, flexural bond, and anchorage lengths of different FRP reinforcements. In addition, they show the differences between different theoretical models for calculating transfer, flexural bond, and anchorage lengths. The theoretical model proposed by (Mahmoud, 1997; Mahmoud et al., 1999), is presented in Figures 4 and 5 with the coefficients α_t taken from (Jokūbaitis & Valivonis, 2022) and the coefficients α_{fb} proposed in this article (Table 4).

In Jokūbaitis & Valivonis (2022), a detailed comparison of the experimental and theoretical transfer length results (more than 300) is provided for different types of FRP reinforcement. Despite the lower number of transfer length results of CFCC, CFRP, and AFRP reinforcement analyzed in this article, it is evident that the tendency of comparison of the experimental and theoretical results is similar to that provided in Jokūbaitis & Valivonis (2022) (Figures 4a, 5a and 6d).

In the case of CFCC strands (Figure 4b), Equations (8), (9), and (10) give the most inappropriate results with a significant overestimation of the experimental flexural bond length results with $L_{fb,teor}/L_{fb.exp} = 4.2$, STD = 1.21, COV = 28.7%; $L_{fb,teor}/L_{fb.exp} = 5.6$, STD = 1.62, COV = 28.7%; and $L_{fb,teor}/L_{fb.exp} = 4.5$, STD = 1.0, COV = 21.9%, respectively (Figure 4b). A similar tendency is observed for the anchorage length of the CFCC strands (Figure 4c).

Equation (7) gives an overestimation of 8% of the experimental results of flexural bond length ($L_{fb,teor}/L_{fb.exp} = 0.92$, STD = 0.21, COV = 22.7%) (Figure 4b). However, the experimental results on anchorage length are more overestimated ($L_{a,teor}/L_{a.exp} = 0.83$, STD = 0.17, COV = 22.0%) (Figure 4c). This is due to the 25% higher experimental transfer length results (Equation 2) with respect to the theoretical results ($L_{t,teor}/L_{t.exp} = 0.75$, STD = 0.15, COV = 22.0%) (Figure 4a). Equations (2) and (7) were proposed for the CFCC

strands (Domenico, 1995; Domenico et al., 1998). However, the results of the larger database showed that its accuracy is not sufficient.

Equations (1) and (6) with the proposed values of coefficients α_t = 4.8 (Jokūbaitis et al., 2022; Mahmoud, 1997; Mahmoud et al., 1999) and α_{fb} = 3.0 gave the most accurate prediction of the transfer and flexural bond lengths (Figure 4a and 4b) ($L_{t,teor}/L_{t.exp}$ = 1.03, STD = 0.14, COV = 13.6% and $L_{fb,teor}/L_{fb.exp}$ = 1.0, STD = 0.20, COV = 19.7%), respectively. Therefore, the prediction of anchorage length was also very accurate ($L_{a,teor}/L_{a.exp}$ = 1.03, STD = 0.13, COV = 12.9%) (Figure 4c).

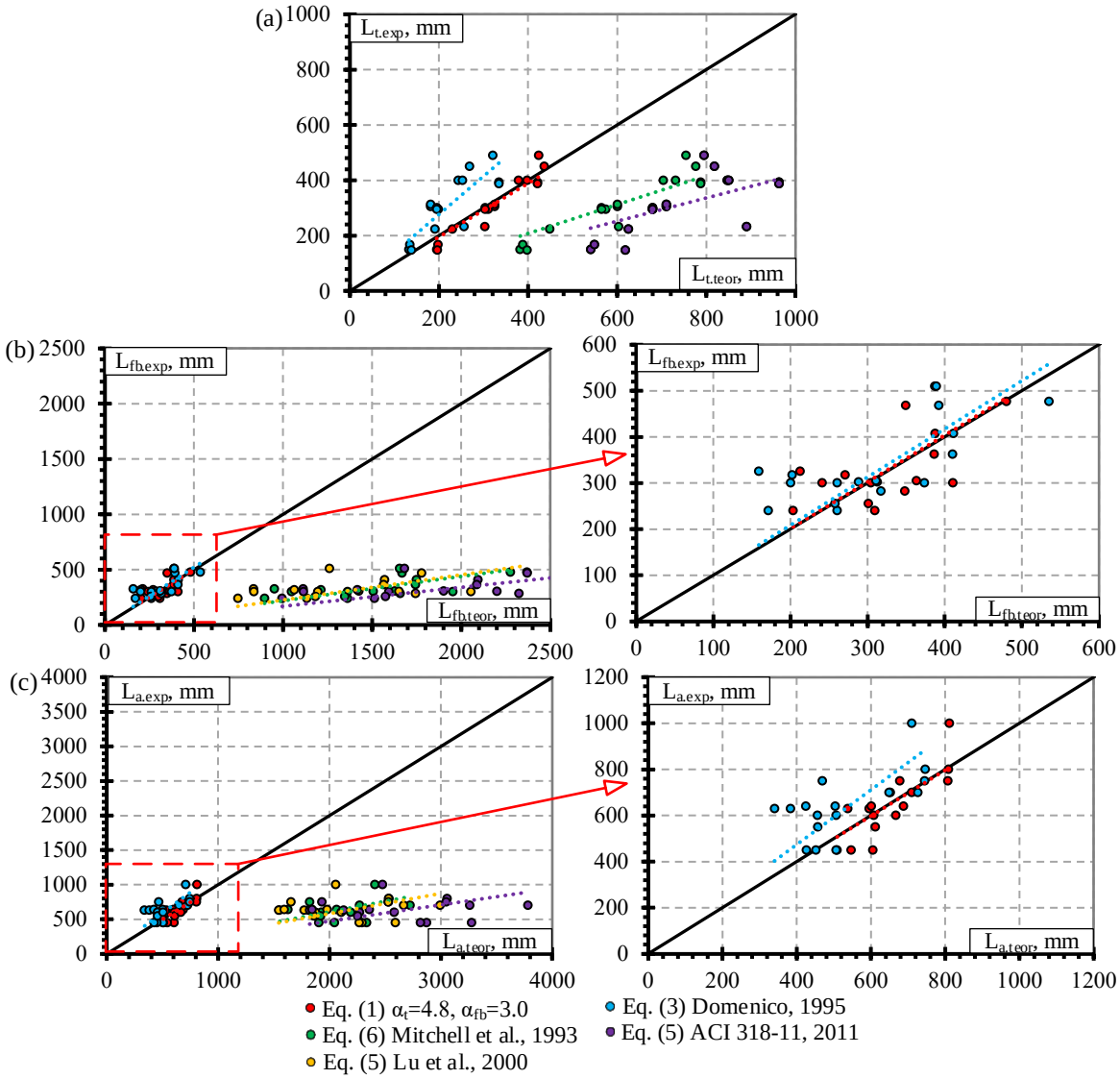

Figure 4. Relationship between the experimental and theoretical (a) transfer length, (b) flexural bond length and (c) anchorage length of CFCC strands

The prediction of the experimental results of the flexural bond and anchorage length of the CFRP bars is significantly underestimated according to Equation (7) with $L_{fb,teor}/L_{fb.exp}$ = 0.35, STD = 0.10, COV = 28.6% (Figure 5b) and $L_{a,teor}/L_{a.exp}$ = 0.37, STD = 0.11, COV = 28.9% (Figure 5c), respectively. The same tendency is observed in the case of the AFRP bars with $L_{fb,teor}/L_{fb.exp}$ = 0.30, STD = 0.09, COV = 29.0% (Figure 5e) and $L_{a,teor}/L_{a.exp}$ = 0.31, STD = 0.07, COV = 22.8% (Figure 5f).

The flexural bond (Figures 5b and 5e) and anchorage (Figures 5c and f) length results of prestressed CFRP bars determined according to the theoretical models of (Lu et al., 2000) and (Mitchell et al., 1993) are similar. However, it overestimates the experimental results of flexural bond length with $L_{fb,teor}/L_{fb.exp}$ = 1.38, STD = 0.32, COV = 22.9% and $L_{fb,teor}/L_{fb.exp}$ = 1.39, STD = 0.32, COV = 23.1%, respectively (Figure 5b) and the anchorage

length with $L_{a,teor}/L_{a.exp}$ = 1.28, STD = 0.25, COV = 19.4% and $L_{a,teor}/L_{a.exp}$ = 1.18, STD = 0.22, COV = 18.4%, respectively (Figure 5c). Even higher overestimation of experimental flexural bond and anchorage length results of prestressed AFRP bars determined according to the theoretical models of (Lu et al., 2000) and (Mitchell et al., 1993) can be seen in Figures 5e and f. Therefore, $L_{fb,teor}/L_{fb.exp}$ = 1.50, STD = 0.31, COV = 20.9% and $L_{fb,teor}/L_{fb.exp}$ = 1.62, STD = 0.36, COV = 22.2%, respectively (Figure 5e) and $L_{a,teor}/L_{a.exp}$ = 1.40, STD = 0.30, COV = 21.2% and $L_{a,teor}/L_{a.exp}$ = 1.39, STD = 0.33, COV = 23.9%, respectively (Figure 5f).

The highest difference between the experimental and theoretical flexural bond and anchorage length results of CFRP and AFRP bars was observed according to the theoretical model provided in (ACI 318-11, 2011). An overestimation of experimental flexural bond length results is up to 85% with STD = 0.42, COV = 22.9% and 100% with STD = 0.42, COV = 20.9% for CFRP and AFRP bars, respectively (Figure 5b and e). In addition, an overestimation of the experimental anchorage length results is up to 57% with STD = 0.33, COV = 21.3% and 71% with STD = 0.38, COV = 22.4% for CFRP and AFRP bars, respectively (Figure 5c and f).

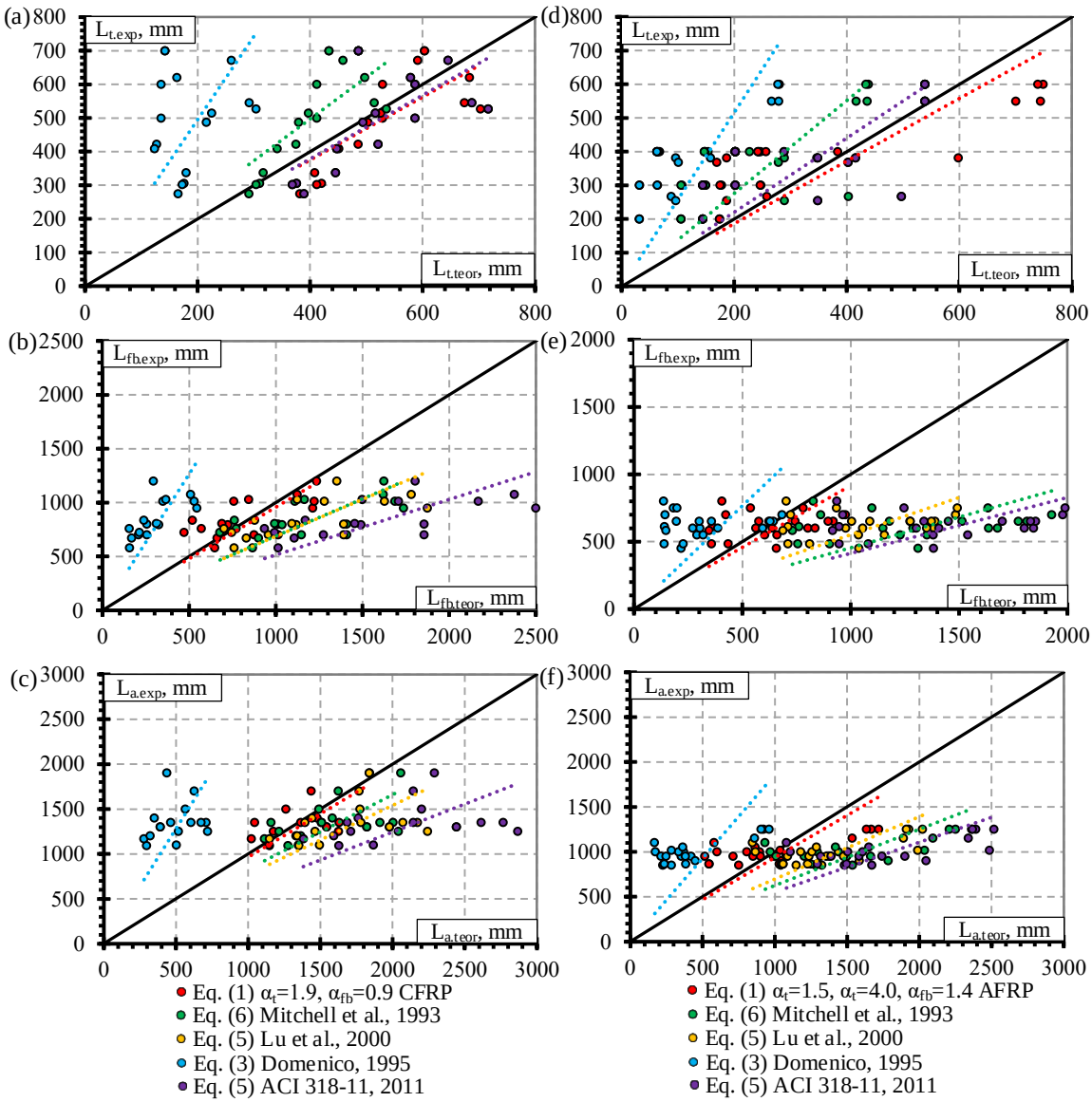

Figure 5. Relationship between experimental and theoretical (a) transfer, (b) flexural bond and (c) anchorage length of CFRP bars and (d) transfer, (e) flexural bond and (f) anchorage length of AFRP bars

The proposed coefficients α_{fb} = 0.9 and α_{fb} = 1.4 for the flexural bond lengths of the CFRP and AFRP bars, respectively, gave the most accurate prediction of the experimental results ($L_{fb,teor}/L_{fb.exp}$ = 1.0, STD = 0.24, COV = 24.0% (Figure 5b) and $L_{fb,teor}/L_{fb.exp}$ = 1.02, STD = 0.30, COV = 29.8% (Figure 5e), respectively) by applying the theoretical model proposed by (Mahmoud, 1997; Mahmoud et al., 1999). In addition, the

combination of the proposed coefficients $\alpha_t = 1.9$, $\alpha_t = 2.9$ (Jokūbaitis et al., 2022) and $\alpha_{fb} = 0.9$, $\alpha_{fb} = 1.4$ (Equations 1 and 6) gives the most accurate prediction of anchorage length of CFRP and AFRP bars, respectively with $L_{a,teor}/L_{a.exp} = 1.03$, STD = 0.15, COV = 14.1% (Figure 5c) and $L_{a,teor}/L_{a.exp} = 0.95$, STD = 0.27, COV = 28.7%, respectively (Figure 5f). Comparison of the ratio between theoretical and experimental results of the transfer length ($L_{t.teor}/L_{t.exp}$), flexural bond length ($L_{fb.teor}/L_{fb.exp}$) and anchorage length ($L_{a.teor}/L_{a.exp}$) of the CFCC strands, CFRP and AFRP bars with different values of coefficients α_t and α_{fb} is presented in Figures 6, 7 and 8, respectively. In Jokūbaitis & Valivonis (2022), it was confirmed that the coefficients $\alpha_t = 1.9$ and $\alpha_t = 4.8$ proposed by other authors are suitable for predicting the transfer length of the CFRP bars, and CFCC strands (only gradual type of release), respectively. Additionally, new values of coefficient α_t were proposed for smooth braided AFRP bars ($\alpha_t = 1.9$) and for sanded and rough AFRP bars $\alpha_t = 4.0$.

The coefficient α_t (used in Equation (1)) was proposed for CFCC strands and CFRP bars (Mahmoud, 1997; Mahmoud et al., 1999) (Table 2) and validated with a larger database of the transfer length results in (Jokūbaitis et al., 2022). Additionally, in Jokūbaitis et al. (2022), new values of coefficient α_t were proposed for the transfer length of smooth braided AFRP bars ($\alpha_t = 1.9$) and for sanded and rough AFRP bars ($\alpha_t = 4.0$). Therefore, these values are used for the comparison of theoretical and experimental transfer length results of the CFCC strands (Figure 6a), CFRP bars (Figure 7a), and AFRP bars (Figure 8a). The results showed sufficiently good agreement between theoretical and experimental transfer lengths with $L_{t.teor}/L_{t.exp} = 1.03$, STD = 0.14, COV = 13.6% for CFCC strands (Figure 6a), $L_{t.teor}/L_{t.exp} = 1.11$, STD = 0.18, COV = 16.4% for CFRP bars (Figure 7a) and $L_{t.teor}/L_{t.exp} = 0.86$, STD = 0.31, COV = 36.0% for AFRP bars (Figure 8a). The 14% underestimation of the experimental transfer length results of AFRP bars could be related to a lower number of specimens analyzed in this article (21 specimens) and the high variation of the transfer length results reported in Jokūbaitis et al., (2022).

Different values of the coefficient α_{fb} (used in Equation (6)) were proposed by other authors and determined in this article (Table 4). The proposed value of $\alpha_{fb} = 3.0$ for the flexural bond length of the CFCC strands is slightly higher compared to $\alpha_{fb} = 2.8$ (Mahmoud, 1997; Mahmoud et al., 1999). For the CFCC strand, the proposed value of $\alpha_{fb} = 3.0$ gives better agreement with the experimental results of flexural bond length ($L_{fb.teor}/L_{fb.exp} = 1.0$, STD = 0.19, COV = 19.7%) compared to the theoretical results higher by 8% ($L_{fb.teor}/L_{fb.exp} = 1.08$, STD = 0.22, COV = 20.5%) with $\alpha_{fb} = 2.8$ (Figure 6b). Additionally, the linear trend line presented in Figure 6b shows that the theoretical results with $\alpha_{fb} = 3.0$ are in closer agreement with the experimental flexural bond length. Furthermore, the combination of $\alpha_t = 4.8$ and $\alpha_{fb} = 3.0$ gives better agreement with the experimental anchorage length results of the CFCC strands ($L_{a.teor}/L_{a.exp} = 1.03$, STD = 0.13, COV = 12.9%) compared to the combination of $\alpha_t = 4.8$ and $\alpha_{fb} = 2.8$ ($L_{a.teor}/L_{a.exp} = 1.08$, STD = 0.15, COV = 13.5%) (Figure 6c).

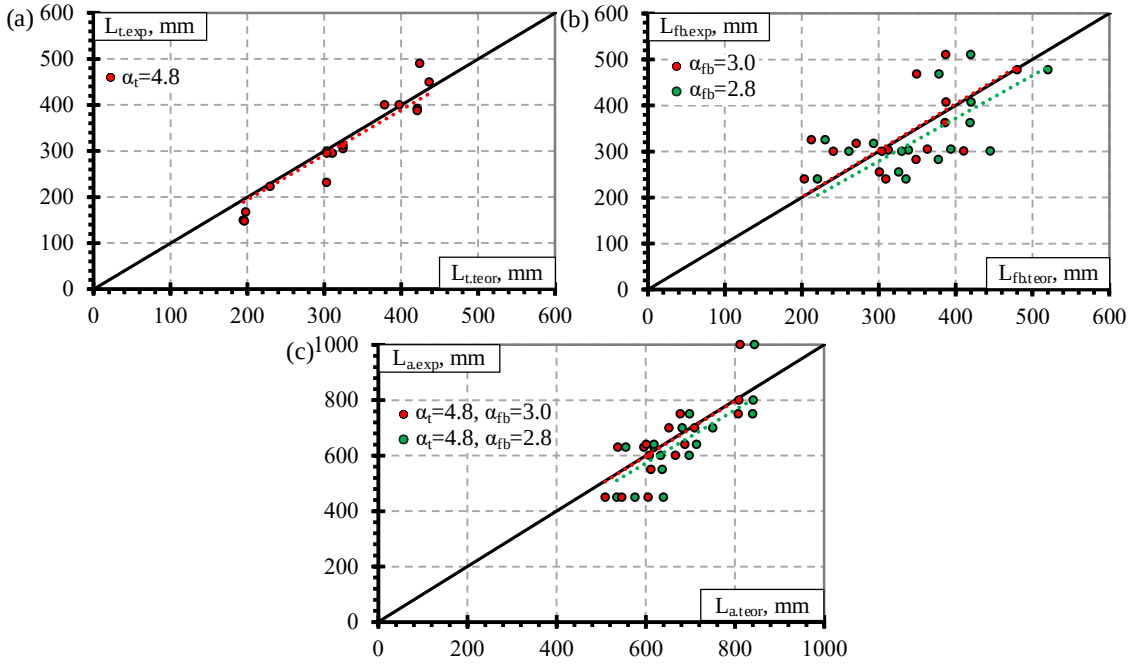

Figure 6. Comparison of experimental and theoretical (a) transfer, (b) flexural bond and (c) anchorage length results of prestressed CFCC strands

The proposed value of α_{fb} = 0.9 for the flexural bond length of CFRP bars agrees better with the experimental results ($L_{fb.teor}/L_{fb.exp}$ = 1.0, STD = 0.24, COV = 24.0%) compared to the theoretical results lower by 9% ($L_{fb.teor}/L_{fb.exp}$ = 0.91, STD = 0.22, COV = 24.0%) with α_{fb} = 1.0 (Mahmoud, 1997; Mahmoud et al., 1999) (Figure 7b). It shows that the theoretical results of the flexural bond length with α_{fb} = 0.9 are higher compared to the results with α_{fb} = 1.0 and therefore are on the safe side. Additionally, the combination of α_t = 1.9 and α_{fb} = 0.9 gives better agreement with the experimental anchorage length results of CFRP bars ($L_{a.teor}/L_{a.exp}$ = 1.03, STD = 0.14, COV = 14.1%) compared to the combination of α_t = 1.9 and α_{fb} = 1.0 ($L_{a.teor}/L_{a.exp}$ = 0.97, STD = 0.13, COV = 13.6%) (Figure 7c).

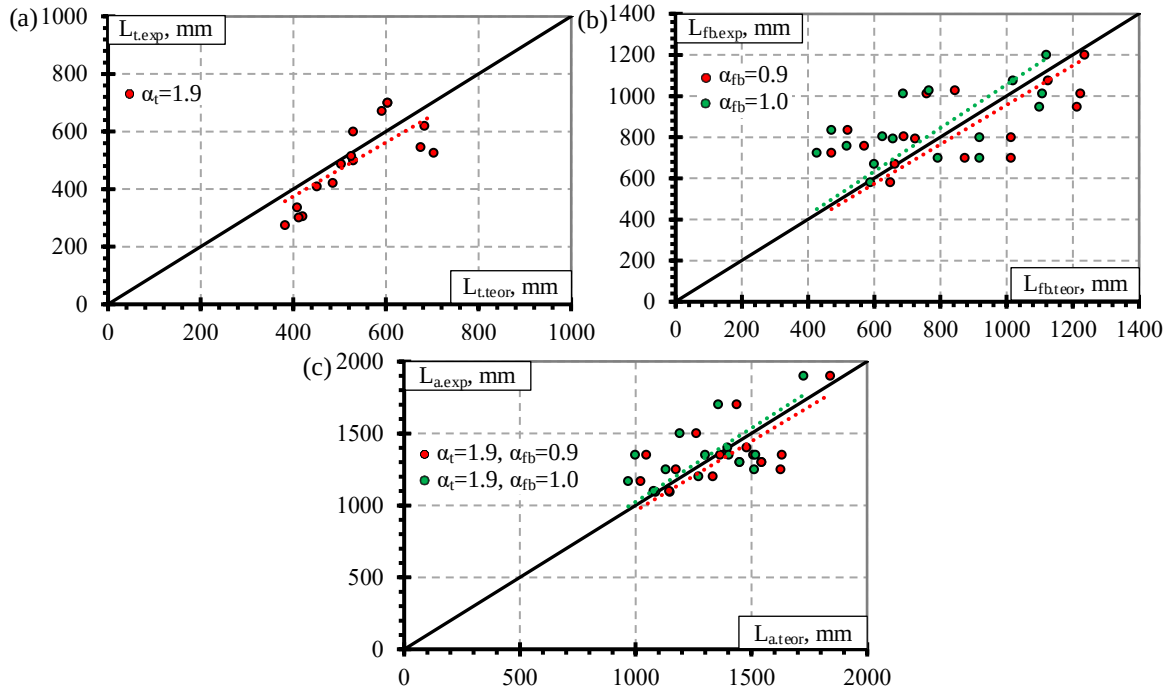

Figure 7. Comparison of experimental and theoretical (a) transfer, (b) flexural bond and (c) anchorage length results of prestressed CFRP bars

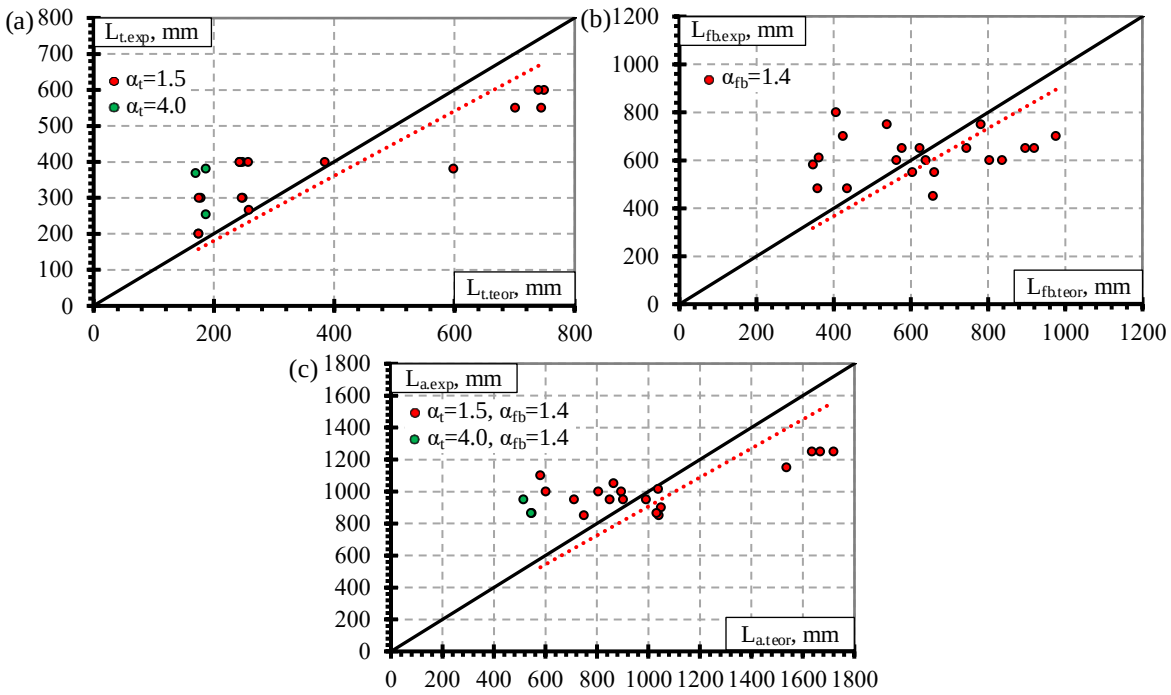

Figure 8. Comparison of experimental and theoretical (a) transfer, (b) flexural bond and (c) anchorage length results of prestressed AFRP bars

The literature review does not provide any proposition of α_{fb} for the flexural bond length of AFRP reinforcement. Therefore, in this article, the value of $\alpha_{fb} = 1.4$ is proposed (Table 4) for the flexural bond length of the AFRP bars with $L_{fb.teor}/L_{fb.exp} = 1.02$, STD = 0.30, COV = 29.8% (Figure 8b). In addition, a combination of $\alpha_t = 2.9$ and $\alpha_{fb} = 1.4$ gives good agreement with the experimental anchorage length results of the AFRP bars ($L_{a.teor}/L_{a.exp} = 0.95$, STD = 0.27, COV = 28.7%) (Figure 8c).

The variation of the flexural bond and anchorage length results is highest for AFRP bars compared to CFCC strands and CFRP bars. However, a combination of $\alpha_t = 1.5$ (for smooth braided AFRP bars), $\alpha_t = 4.0$ (for rough and sanded AFRP bars), and $\alpha_{fb} = 1.4$ gives a significantly lower variation of flexural bond and anchorage length compared to the transfer length of the AFRP bars presented in (Jokūbaitis & Valivonis, 2022).

Conclusions

A large database of the transfer, flexural bond and anchorage lengths of different FRP reinforcements was collected, and the analysis of experimental results, description of theoretical models, and comparison of experimental and theoretical results led to the following conclusions and proposals:

The database analysis revealed that the coefficients $\alpha_t = 4.8$, $\alpha_t = 1.9$, $\alpha_t = 1.5$, and $\alpha_t = 4.0$ proposed in the literature are suitable for predicting the transfer length of the CFCC strands, CFRP bars, AFRP bars with smooth braided surface and AFRP bars with rough and sanded surface, respectively. The analysis of the results of a larger database in this article shows that the coefficients $\alpha_{fb} = 2.8$ and $\alpha_{fb} = 1.0$ proposed by other authors for the flexural bond length of CFCC strands and CFRP bars, respectively, should be corrected. Therefore, the corrected values of $\alpha_{fb} = 3.0$ for CFCC strands (for concrete strength 31–64 MPa, stresses in reinforcement 735–1306 MPa, and reinforcement diameter 10.5–15.2 mm) and $\alpha_{fb} = 0.9$ for CFRP bars (for concrete strength 37–71 MPa, stresses in reinforcement 535–1400 MPa and reinforcement diameter 7.9–12.7 mm) are proposed, respectively. In addition, Equation (6) was determined to give the most accurate prediction of the flexural bond length by applying the proposed α_{fb} values for different types of FRP reinforcement.

The database is too small to clearly define the influence of different surface conditions of AFRP bars on the flexural bond length. Therefore, the new general value of the coefficient $\alpha_{fb} = 1.4$ was proposed for the prediction of the flexural bond length of the AFRP bars. The proposed value is valid for a concrete strength 31–47 MPa, stresses in reinforcement 258–1061 MPa, and reinforcement diameter 7.4–16 mm.

The combination of coefficients α_t proposed in the literature ($\alpha_t = 4.8$ for CFCC strands, $\alpha_t = 1.9$ for CFRP bars, $\alpha_t = 1.5$ for AFRP bars with smooth braided surface and $\alpha_t = 4.0$ for AFRP bars with rough and sanded surface) and coefficients α_{fb} proposed in this article ($\alpha_{fb} = 3.0$ for CFCC strands, $\alpha_{fb} = 0.9$ for CFRP bars and $\alpha_{fb} = 1.4$ for AFRP bars) for the prediction of the anchorage length of different FRP reinforcement according to Equations (1) and (6) gives the most accurate results.

The analysis of the flexural bond and anchorage length and the new values proposed for the coefficient α_{fb} provides possibilities for adapting it to design codes for engineering applications and performing additional research that fills the missing gaps in the field. In particular, additional research is needed on the effects of shear reinforcement of CFCC strands, CFRP and AFRP bars, and the surface conditions of the AFRP and CFRP bars. Furthermore, the prediction of flexural bond and anchorage length of BFRP reinforcement could be a subject of future research.

Scientific Ethics Declaration

The authors declare that the scientific, ethical, and legal responsibility of this article published in EPSTEM journal belongs to the authors.

Acknowledgements

* This article was presented as an oral presentation at the International Conference on Technology, Engineering and Science (www.icontes.net) held in Antalya/Turkey on November 16-19, 2022.

* This research was funded by the European Social Fund (project No 09.3.3-LMT-K-712-23-0161) under a grant agreement with the Research Council of Lithuania (LMTLT).

References

ACI 318-11, Committee 318, & American Concrete Institute. (2011). *ACI 318-11. Building code requirements for structural concrete (ACI 318-11) and commentary*. American Concrete Institute.

ACI 404.4R-04, Committee 440, & American Concrete Institute. (2004). *ACI 404.4R-04. Prestressing concrete structures with FRP tendons*. American Concrete Institute.

Atutis, E., Valivonis, J., & Atutis, M. (2018). Experimental study of concrete beams prestressed with basalt fiber reinforced polymers under cyclic load. *Composite Structures, 183*(1), 389–396. https://doi.org/10.1016/j.compstruct.2017.03.106

Atutis, M., Valivonis, J., & Atutis, E. (2018). Experimental study of concrete beams prestressed with basalt fiber reinforced polymers. Part I: Flexural behavior and serviceability. *Composite Structures, 183*(1), 114–123. https://doi.org/10.1016/j.compstruct.2017.01.081

CAN-CSA S806-12, & Canadian Standards Association. (2012). *CAN-CSA S806-12. Design and construction of building structures with fibre-reinforced polymers.* https://www.csagroup.org/store/product/S806-12/

Dolan, C. W., Hamilton, H. R. III., Bakis, C. E., & Nanni, A. (2001). Design recommendations for concrete structures prestressed with FRP tendons. FHWA Contract. DTFH61-96-C-00019. Final Report. http://wwweng.uwyo.edu/civil/research/papers/.

Domenico, N. G. (1995). Bond properties of CFCC prestressing strands in pretensioned concrete beams [Master Thesis]. University of Manitoba.

Domenico, N. G., Mahmoud, Z. I., & Rizkalla, S. H. (1998). Bond properties of carbon fiber composite prestressing strands. *ACI Structural Journal, 95*(3), 281–290.

Ehsani, M. R., Saadatmanesh, H., & Nelson, C. T. (1997). Transfer and flexural bond performance of aramid and carbon frp tendons. *PCI Journal, 42*(1), 76–86. https://doi.org/10.15554/pcij.01011997.76.86

EN 1992-1-1. (2004). *EN 1992-1-1 Eurocode 2. Design of concrete structures. Part 1-1: General rules and rules for buildings*. European Committee for Standardization. https://www.phd.eng.br/wp-content/uploads/2015/12/en.1992.1.1.2004.pdf

Jokūbaitis, A., Marčiukaitis, G., & Valivonis, J. (2016). Influence of technological and environmental factors on the behaviour of the reinforcement anchorage zone of prestressed concrete sleepers. *Construction and Building Materials, 121*, 507–518. https://doi.org/10.1016/j.conbuildmat.2016.06.025

Jokūbaitis, A., Marčiukaitis, G., & Valivonis, J. (2017). Analysis of reinforcement anchorage zone behavior of prestressed concrete elements under static and cyclic loads. *Procedia Engineering, 172*, 457–464. https://doi.org/10.1016/j.proeng.2017.02.028

Jokūbaitis, A., Marčiukaitis, G., & Valivonis, J. (2020a). Bond of bundled strands under static and cyclic load and freezing-thawing effect. *Engineering Structures, 208*, 1–11. https://doi.org/10.1016/j.engstruct.2019.109922

Jokūbaitis, A., Marčiukaitis, G., & Valivonis, J. (2020b). Experimental research on the behavior of the rail seat section of different types of prestressed concrete sleepers. *Materials, 13*(11), 1–22. https://doi.org/10.3390/ma13112432

Jokūbaitis, A., Marčiukaitis, G., Valivonis, J., & Strauss, A. (2018). Influence of cyclic loading and frost on the behavior of bond of three-wire strand. *Structural Concrete, 19*(5), 1363–1375. https://doi.org/10.1002/suco.201700245

Jokūbaitis, A., & Valivonis, J. (2022). An analysis of the transfer lengths of different types of prestressed fiber-reinforced polymer reinforcement. *Polymers, 14*(19), 3931. https://doi.org/10.3390/polym14193931

Jokūbaitis, A., Valivonis, J., & Marčiukaitis, G. (2016). Analysis of strain state and cracking of concrete sleepers. *Journal of Civil Engineering and Management, 22*(4), 564–572. https://doi.org/10.3846/13923730.2016.1147494

Krem, S. (2013). Bond and flexural behaviour of self consolidating concrete beams reinforced and prestressed with FRP Bars [PhD Thesis]. University of Waterloo.

Krem, S. S., & Soudki, K. A. (2018). Bond behaviour of CFRP bars prestressed in self-consolidating concrete beams. *ACI Symposium Paper, 327*, 1–20.

Lu, Z., Boothby, T. E., Bakis, C. E., & Nanni, A. (2000). Transfer and development lengths of FRP prestressing tendons. *PCI Journal, 45*(2), 84–95. https://doi.org/10.15554/pcij.03012000.84.95

Mahmoud, Z. I. (1997). Bond characteristics of fibre reinforced polymers prestressing reinforcement [PhD Thesis]. Alexandria University.

Mahmoud, Z. I., Rizkalla, S. H., & Zaghoul, E. E. R. (1999). Transfer and development lengths of carbon fiber reinforced polymers prestressing reinforcement. *ACI Structural Journal, 96*(4), 594–602.

MC 1990, & Comite Euro-International du Beton. (1991). *CEB-FIP Model Code 1990*. Thomas Telford.

MC 2010, & Internationa Federation of Structural Concrete. (2012). *fib Bulletin 65: Model Code 2010,* Final draft. Ernst & Sohn.

Mitchell, D., Cook, W. D., & Tham, T. (1993). Influence of high strength concrete on transfer and development length of pretensioning strand. *PCI Journal, 38*(3), 52–66. https://doi.org/10.15554/pcij.05011993.52.66

Nanni, A., & Tanigaki, M. (1992). Pretensioned prestressed concrete members with bonded fiber reinforced plastic tendons: Development and flexural bond lengths (Static). *ACI Structural Journal, 89*(4), 433–441.

Nanni, A., Utsunomiya, T., Yonekura, H., & Tanigaki, M. (1992). Transmission of prestressing force to concrete by bonded fiber reinforced plastic tendons. *ACI Structural Journal, 89*(3), 335–344.

Wang, L., Zhang, J., Xu, J., & Han, Q. (2018). Anchorage systems of CFRP cables in cable structures—A review. *Construction and Building Materials, 160*, 82–99. https://doi.org/10.1016/j.conbuildmat.2017.10.134

Author Information

Aidas Jokūbaitis
Department of Reinforced Concrete Structures and Geotechnics,
Faculty of Civil Engineering,
Vilnius Gediminas Technical University
Sauletekio av. 11, LT-10223 Vilnius, Lithuania
Contact e-mail: *aidas.jokubaitis@vilniustech.lt*

Juozas Valivonis
Department of Reinforced Concrete Structures and Geotechnics,
Faculty of Civil Engineering,
Vilnius Gediminas Technical University
Sauletekio av. 11, LT-10223 Vilnius, Lithuania

To cite this article:

Jokubaitis, A. & Valivonis, J. (2022). An analysis of flexural bond length and anchorage length of prestressed fiber reinforced polymer reinforcement. *The Eurasia Proceedings of Science, Technology, Engineering & Mathematics (EPSTEM), 21,* 484-499.

Appendix A

Table A1. Experimental data of prestressed CFCC strands

References	Specimen No	FRP Type	FRP Surface	Specimen Type	Shear Reinforcement	c, mm	Ø, mm	A_p, mm^2	E_p, GPa	f_c, MPa	f_{se}, MPa	f_{pu}, MPa	L_t, mm	L_{fb}, mm	L_a, mm	Mode of failure
(Domenico, 1995; Domenico et al., 1998)	B6	CFCC 7-wire Strand	Helical plain	T Beam	Yes	50	12.5	76	137	68.3	848	2632	126.5	573.5	700	Rupture
	B7			T Beam	Yes	50	12.5	76	137	68.3	875	2674	148.5	401.5	550	Rupture
	B8			T Beam	Yes	50	12.5	76	137	59	794	2305	149.5	300.5	450	Shear/bond slip
	D10			T Beam	Yes	75	12.5	76	137	59	837	2120	167.5	282.5	450	Shear/bond slip
	C9			T Beam	Yes	50	12.5	76	137	64	905	2120	147.5	302.5	450	Shear/bond slip
	BT7			Beam	Yes	50	12.5	76	137	37	1285	2120	400	240.0	640	Bond slip
	BT8			Beam	Yes	50	12.5	76	137	37	1244	2120	375	225.0	600	Bond slip
	A3			T Beam	Yes	50	15.2	113.6	137	57.8	734	2168	223	477.0	700	Bond slip
	D5			T Beam	Yes	75	15.2	113.6	137	57.8	809	2150	200.5	499.5	700	Rupture
	C4			T Beam	Yes	50	15.2	113.6	137	60.5	1074	2150	232	468.0	700	Shear/bond slip
(Mahmoud, 1997; Mahmoud et al., 1999)	BT11	CFCC 7-wire Strand	Helical plain	Beam	Yes	45	10.5	55.7	140	41	1203	1934	305	325.0	630	Rupture
	BT12			Beam	Yes	45	10.5	55.7	140	41	1200	1577	312.5	217.5	530	Bond slip
	BT13			Beam	Yes	45.0	10.5	55.7	140	41	1237	2168	312.5	317.5	630	Bond slip
	BT14			Beam	Yes	45.0	10.5	55.7	140	41	1237	1906	312.5	267.5	580	Bond slip
	BT7			Beam	Yes	50.0	12.5	76.0	141	37	1306	1855	400.0	240.0	640	Bond slip
	BT8			Beam	Yes	50.0	12.5	76.0	141	37	1300	1815	375.0	225.0	600	Bond slip
	BT9			Beam	Yes	50.0	12.5	76.0	141	37	1290	1700	360.0	190.0	550	Bond slip
	BT10			Beam	Yes	50.0	12.5	76.0	141	37	1310	1616	360.0	140.0	500	Bond slip
	BT15a			Beam	Yes	49.0	12.5	76.0	141	41	1000	1924	300.0	400.0	700	Rupture
	BT15b			Beam	Yes	50.0	12.5	76.0	141	41	1000	1879	300.0	300.0	600	Rupture
	BT16a			Beam	Yes	49.0	12.5	76.0	141	41	984	1853	295.0	255.0	550	Bond slip
	BT16b			Beam	Yes	50.0	12.5	76.0	141	41	984	2033	295.0	305.0	600	Rupture
	BT19			Beam	No	50.0	12.5	76.0	141	34	1215	2100	500.0	450.0	950	Rupture
	BT20			Beam	No	50.0	12.5	76.0	141	34	1215	1830	450.0	300.0	750	Rupture
	BT1			Beam	Yes	60.0	15.2	113.6	138	46	905	1814	365.0	435.0	800	Bond slip
	BT2			Beam	Yes	60.0	15.2	113.6	138	46	905	1916	355.0	445.0	800	Bond slip
	BT3			Beam	Yes	60.0	15.2	113.6	138	43	1200	2150	392.5	407.5	800	Rupture
	BT4			Beam	Yes	60.0	15.2	113.6	138	43	1223	2170	387.5	362.5	750	Slip/rupture
	BT5			Beam	Yes	60.0	15.2	113.6	138	43	1232	1756	400.0	200.0	600	Bond slip
	BT6			Beam	Yes	60.0	15.2	113.6	138	43	1223	1720	400.0	200.0	600	Bond slip
	BT17a			Beam	No	59.0	15.2	113.6	138	33	1165	1600	650.0	250.0	900	Bond slip
	BT17b			Beam	No	60.0	15.2	113.6	138	33	1165	1744	650.0	450.0	1100	Bond slip
	BT18			Beam	No	60.0	15.2	113.6	138	33	1170	1932	600.0	650.0	1250	Bond slip
	BT21			Beam	No	60.0	15.2	113.6	138	31	979	2260	510.0	840.0	1350	Rupture
	BT22a			Beam	No	59.0	15.2	113.6	138	31	971	1734	490.0	510.0	1000	Slip/rupture
	BT22b			Beam	No	60.0	15.2	113.6	138	31	971	1618	490.0	410.0	900	Bond slip

Table A2. Experimental data of prestressed CFRP bars

References	Specimen No	FRP Type	FRP Surface	Specimen Type	Shear Reinforcement	c, mm	O, mm	A_p, mm^2	E_p, GPa	f_c, MPa	f_{se}, MPa	f_{pu}, MPa	L_t, mm	L_{fb}, mm	L_a, mm	Mode of failure
(Lu et al., 2000)	CL	CFRP Leadline tendon	Spirally Indented	Beam	No	40.6	7.9	47.1	171	45.4	1241	2208	421.6	670.4	1092	
	CS			Beam	No	40.6	7.9	50.3	161	44.1	1006.6	1823	408.9	758.1	1167	
(Mahmoud, 1997; Mahmoud et al., 1999)	BL1	CFRP Leadline tendon	Spirally Indented	Beam	Yes	35.0	8.0	46.1	147	50	1068	1870	452.5	347.5	800	Bond slip
	BL2			Beam	Yes	35.0	8.0	46.1	147	50	1078	1850	462.5	337.5	800	Bond slip
	BL3			Beam	Yes	35.0	8.0	46.1	147	46	1082	1753	480	320	800	Bond slip
	BL4			Beam	Yes	35.0	8.0	46.1	147	46	1082	1764	480	320	800	Bond slip
	BL5			Beam	Yes	35.0	8.0	46.1	147	41	1255	2129	620	580	1200	Bond slip
	BL6			Beam	Yes	35.0	8.0	46.1	147	41	1227	1420	625	175	800	Bond slip
	BL7			Beam	Yes	35.0	8.0	46.1	147	41	1248	1820	610	390	1000	Bond slip
	BL8			Beam	Yes	35.0	8.0	46.1	147	41	1248	1700	625	375	1000	Bond slip
	BL9			Beam	No	36.0	8.0	46.1	147	37	1100	2655	700	1200	1900	Rupture
	BL10			Beam	No	36.0	8.0	46.1	147	37	1100	2200	700	700	1400	Bond slip
	BL11			Beam	No	36.0	8.0	46.1	147	52	1400	3000	600	700	1300	Slip/rupture
	BL12a			Beam	No	36.0	8.0	46.1	147	52	1365	2770	500	600	1100	Bond slip
	BL12b			Beam	No	36.0	8.0	46.1	147	52	1365	2965	500	800	1300	Rupture
	PL1			Prism	No	35.0	8.0	46.1	147	34	1123	1777	490	260	750	Bond slip
	PL2			Prism	No	35.0	8.0	46.1	147	34	1123	1247	480	270	750	Bond slip
	PL3			Prism	No	40.0	8.0	46.1	147	31	1340	2073	540	210	750	Bond slip
	PL4			Prism	No	40.0	8.0	46.1	147	31	1340	2311	525	225	750	Slip/rupture
(Ehsani et al., 1997)	CL-1 (J)	CFRP Leadline tendon	Spirally Indented	Beam	No	64.7	7.9	46.5	150	46	1013	1847	432	965	1397	Bond slip
(Krem, 2013; Krem et al., 2018)	I-SCC30-1	CFRP Bar	Sanded	Beam	Yes	38.1	12.7	126.7	144	62.1	549	1360	306	794	1100	Pullout
	I-SCC30-2			Beam	Yes	38.1	12.7	126.7	144	62.1	534	1892	302	948	1250	Rupture
	I-SCC30-3			Beam	Yes	38.1	12.7	126.7	144	49.6	626	1804	337	1013	1350	Pullout/Rupture
	I-SCC30-4			Beam	Yes	38.1	12.7	126.7	144	49.6	604	1187	320	1180	1500	Rupture
	II-SCC45-1			Beam	Yes	38.1	12.7	126.7	144	70.9	750	1332	534	566	1100	Pullout
	II-SCC45-2			Beam	Yes	38.1	12.7	126.7	144	70.9	794	1509	516	734	1250	Pullout
	II-SCC45-3			Beam	Yes	38.1	12.7	126.7	144	70.9	776	1412	515	835	1350	Pullout
	II-SCC45-4			Beam	Yes	38.1	12.7	126.7	144	70.9	741	1669	487	1013	1500	Rupture
	III-SCC60-1			Beam	Yes	38.1	12.7	126.7	144	62.1	932	1302	669	431	1100	Pullout
	III-SCC60-2			Beam	Yes	38.1	12.7	126.7	144	62.1	995	1473	733	617	1350	Pullout
	III-SCC60-3			Beam	Yes	38.1	12.7	126.7	144	49.6	920	1531	662	838	1500	Pullout
	III-SCC60-4			Beam	Yes	38.1	12.7	126.7	144	49.6	974	1787	672	1028	1700	Pullout/Rupture
	IV-N30-1			Beam	Yes	38.1	12.7	126.7	144	64.5	563	1854	275	1075	1350	Rupture
	IV-N60-2			Beam	Yes	38.1	12.7	126.7	144	64.5	1076	1616	527	723	1250	Pullout
	IV-N60-3			Beam	Yes	38.1	12.7	126.7	144	64.5	1026	1817	545	805	1350	Rupture
	IV-N60-4			Beam	Yes	38.1	12.7	126.7	144	64.5	1052	1859	534	966	1500	Rupture

Table A3. Experimental data of prestressed AFRP bars

References	Specimen No	FRP Type	FRP Surface	Specimen Type	Shear Reinforcement	ς, mm	O, mm	A_p, mm^2	E_p, GPa	f_c, MPa	f_{se}, MPa	f_{pu}, MPa	L_t, mm	L_{fb}, mm	L_s, mm	Mode of failure
(Ehsani et al., 1997)	AA-1 (D)	AFRP Arapee	Smooth	Beam	No	63.7	9.9	38.1	128	44.5	1061	2448	267	749	1016	
	AF-3 (J)	AFRP Fibra	Smooth-braided	Beam	No	63.4	10.4	83.2	48	43	717	1434	381	483	864	
	AT-3 (J)	AFRP Technora	Rough	Beam	No	64.9	7.4	43.2	69	46.4	841	1724	254	610	864	
	AT-3 (D)		Rough	Beam	No	64.9	7.4	43.2	69	47.1	841	1724	381	483	864	
(Lu et al., 2000)	AT	AFRP Technora	Rough	Beam	No	40.6	7.9	50.3	45	47.1	910	1710	368	582	950	
(Nanni et al., 1992; Nanni & Tanigaki, 1992)	A2-1	AFRP Tendon 2-K64	Braided (Smooth)	Beam	No	66	8	42	76	37.4	295	1133	300	650	950	Slip/split crack
	A2-2(J)			Beam	No	66	8	42	76	37.5	295	1126	300	700	1000	Slip/split crack
	A2-2(F)			Beam	No	66	8	42	76	38.4	288	1095	300	800	1100	Crushing/shear failure
	A2-S3(J)			Beam	Yes	66	8	42	76	38.6	288	1362	200	750	950	Crushing/shear failure
	A2-S3(F)			Beam	Yes	66	8	42	76	38.7	288	1442	200	650	850	Slip/split crack
	A2-S4(F)			Beam	Yes	66	8	42	76	33.1	650	1674	400	550	950	Concrete crush
	A2-S4(J)			Beam	Yes	66	8	42	76	33.4	650	1843	400	450	850	Concrete crush
	B1-1(F)	AFRP Tendon 1-K128		Beam	No	64	12	90	68	37.8	272	1163	400	650	1050	Crushing/shear failure
	B1-1(J)			Beam	No	64	12	90	68	37.9	272	1066	400	550	950	Slip/split crack
	B1-2(F)			Beam	No	64	12	90	68	35.8	272	1081	400	600	1000	Crushing/shear failure (slip/split crack)
	B1-2(J)			Beam	No	64	12	90	68	38.6	272	1021	400	600	1000	Crushing/shear failure
	B1-S3(J)			Beam	Yes	64	12	90	68	37.6	276	1271	300	800	1100	Concrete crush
	B1-S3(F)			Beam	Yes	64	12	90	68	37.8	276	1253	300	650	950	Concrete crush
	B1-S6(J)			Beam	Yes	64	12	90	68	38.0	276	1269	300	550	850	Bond slip
	B1-S6(F)			Beam	Yes	64	12	90	68	38.1	276	1336	300	600	900	Slip/split crack
	B1-S7(F)			Beam	Yes	64	12	90	68	33.7	607	1463	450	500	950	Bond slip
	B1-S7(J)			Beam	Yes	64	12	90	68	34.0	607	1525	450	550	1000	Slip/split crack
	B2-S1(J)	AFRP Tendon 2-K128		Beam	Yes	64	12	90	68	38.9	258	1092	400	650	1050	Crushing/shear failure
	B2-S1(F)			Beam	Yes	64	12	90	68	39.0	258	1144	400	550	950	Slip/split crack
	C1-S4(F)	AFRP Tendon 1-K256		Beam	Yes	62	16	180	63	34.3	593	1383	550	500	1050	Slip/split crack
	C1-S4(J)			Beam	Yes	62	16	180	63	34.6	593	1370	550	600	1150	Concrete crush (slip/split crack)
	C1-S6/1			Beam	Yes	62	16	180	63	31.3	607	1406	600	650	1250	Slip/split crack
	C1-S6/2			Beam	Yes	62	16	180	63	31.9	607	1396	600	650	1250	Concrete crush
	C1-S7/1			Beam	Yes	62	16	180	63	31.6	607	1460	550	700	1250	Concrete crush
	C1-S7/2			Beam	Yes	62	16	180	63	32.2	607	1284	550	480	1030	Concrete crush
	D1-1(J)	AFRP Tendon 1-K128S	Sanded	Beam	No	63	13.5	90	68	39.0	565	1347	250	800	1050	Crushing/shear failure
	D1-1(F)			Beam	No	63	13.5	90	68	39.1	565	1272	250	700	950	Crushing/shear failure
	D1-S3(J)			Beam	Yes	63	13.5	90	68	39.2	565	1814	200	650	850	Concrete crush
	D1-S3(F)			Beam	Yes	63	13.5	90	68	39.4	565	1876	200	500	700	Concrete crush